THE COMMISSIONING OF TESS: AN EXPERIMENTAL FACILITY FOR MEASURING THE ELECTRON ENERGY DISTRIBUTION FROM PHOTOCATHODES

L.B. Jones*, R.J. Cash, B.D. Fell, K.J. Middleman, T.C.Q. Noakes & B.L. Militsyn
STFC Daresbury Laboratory, ASTeC & the Cockcroft Institute, Warrington WA4 4AD, UK

H.E. Scheibler, D.V. Gorshkov & A.S. Terekhov
Institute of Semiconductor Physics, SB RAS, Novosibirsk 630090, Russia

Abstract

ASTeC have developed an instrument to measure the *transverse energy* (ε_{tr}) of electrons emitted from photocathode sources. The instrument ('*TESS*' for *transverse energy spread spectrometer*) is connected to our GaAs photocathode preparation facility (PPF) which is capable of producing photocathodes with quantum efficiencies (*Q.E.*) up to 20 % at 635 nm [1, 2]. TESS is currently being used to study the emission properties of these photocathodes.

The methodology is based on extracting a fA–scale electron beam from a small area of a photocathode source, and allowing it to expand under the influence of its transverse energy component while in flight between the electron source and a detector. Images of the electron emission footprint are analysed to measure the transverse energy distribution curve (TEDC), and the mean transverse energy extracted (MTE) from this.

TESS is compatible with a number of different light sources, so can support measurements on various photocathode materials from the metal and semiconductor families. The system includes a piezo–electric leak valve allowing precision gas dosing to control the degradation state of the photocathode, and therefore its *Q.E.*. The system also supports cathode cooling to LN_2 temperature at 77 K.

The system has been commissioned recently, in collaboration with the Institute of Semiconductor Physics (ISP) at Novosibirsk. We present this TESS commissioning data for photoelectron emission from a GaAs photocathode.

INTRODUCTION

The development of high–performance accelerator drivers for light sources based on Free–Electron Lasers requires technology which delivers a high–brightness electron beam for reasons that are well–documented [3]. Electron beam brightness in an accelerator is fundamentally limited by injector brightness, and this is itself limited by the source beam emittance or the *intrinsic emittance* of the cathode source. Electron beam brightness will be increased significantly by reducing the longitudinal and transverse energy spread in the emitted electrons, thereby creating a *cold beam*.

* lee.jones@stfc.ac.uk

For a bound electron, the component of electron momentum which is parallel to the surface translates into its transverse momentum component on photoemission. This transverse momentum component is directly related to transverse electron energy, and is measurable as the beam emittance at some distance from the source. When using GaAs photocathodes, the upper limit on transverse electron energy is determined by the illumination wavelength, the level of electron affinity and the photocathode temperature. The profile of the measured TEDC itself depends on various elastic and inelastic electron scattering processes at the photocathode–vacuum interface, which are themselves dependent on several factors such as surface roughness, surface diffraction, material structure/crystallinity etc.

The ability to measure this transverse energy, and to make direct comparisons between photocathodes which have been prepared in different ways is therefore a key enabling step towards increasing electron beam brightness.

We have constructed TESS to measure the transverse energy of photoemitted electrons through analysis of the beam footprint recorded after propagation over a known drift distance, with the emission footprint being directly coupled to the source emittance.

TRANSVERSE ENERGY MEASUREMENT

Early published work (circa 1972) suggested that the angular emission cone for photoelectrons from GaAs is small, though later work appeared to imply the opposite [4]. Applying angle–resolved photoelectron spectroscopy to measure this angular distribution for GaAs is challenging as the angular distribution is affected by the specific geometry of the vacuum chamber and experiment itself, so will vary in each installation. Further recent work indicates that GaAs does indeed have a narrow emission cone with a half–angle of only 15 ° relative to the surface normal [5].

However, it is not possible to decouple the effects of an electron's transverse energy component from its emission angle when considering only its transverse displacement in the emission plane from the point of emission. Consequently, data from TESS includes a contribution from the angular emission, and values returned from a TESS measurement are upper limits on the mean transverse energy.

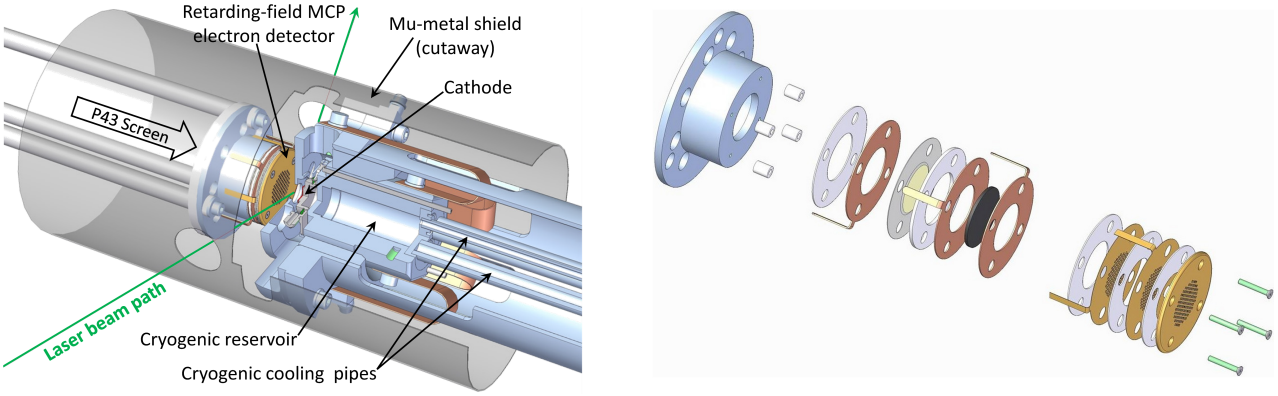

Figure 1: Detail of the TESS experimental system. **Left:** Overview with the vacuum chamber removed and the mu–metal magnetic shield and cathode holder cut away to aid clarity. The cathode holder is to the right, the detector to the left. **Right:** Schematic showing an exploded view of the retarding–field electron detector.

Instrument description

Measurement of the transverse energy component of photoelectrons inevitably leads to working with electrons whose kinetic energies lie between 50 and several hundred eV. This presents challenges due to the detrimental effects of any stray/non–uniform electric and magnetic fields present in the region between the photocathode source and the detector. To counter these effects, the source and detector have been designed to be symmetric and flat, and contain non–magnetic components. Additionally, a mu–metal shield is installed around the source and detector to screen against external magnetic fields.

The TESS system shown in Figure 1 combines a reflection–mode photocathode holder under grazing–incidence illumination with a multi–purpose retarding–field electron detector and imaging system. The photocathode holder can be electrically biased, and can also be cryogenically–cooled permitting measurements to be made on photocathodes cooled to liquid nitrogen temperature.

The electron detector combines three electrically isolated grids with a Hamamatsu F1094-01 2-stage microchannel plate electron multiplier (MCP) and a phosphor screen. The MCP channels are 12 μm ϕ on a 15 μm pitch giving an open area ratio of 60 %. Detail of the detector is shown in Figure 1 (right). The grids are photo–etched from tungsten sheet 35 μm in thickness creating a mesh of pitch 500 μm, then gold–coated to produce non–magnetic assemblies with high electrical conductivity. They are aligned within the detector such that their X- and Y- axes are coincident, and each grid is electrically isolated to a limit of 1 kV. Grid #1 and the detector front plate are engineered to be mechanically flat and electrically common, thereby creating a flat electrical field in the drift space between the source and detector. The MCP front plate floats and can be biased to several hundred volts, and has an active area 20 mm ϕ. The front–back voltage limit is 2 kV which provides a gain approaching 10^7. The phosphor screen is a P43 ITO type (Gd_2O_2S:Tb), 10 to 15 μm in thickness with its peak emission at 543 nm, operable at voltages up to 6 kV. Hamamatsu quote a spatial resolution of 80 to 100 μm for this MCP and screen combination.

The detector assembly is mounted on a Z–translation stage allowing the electron drift distance between the photocathode source and grid #1 to be varied from a minimum around 7.5 mm to a maximum of 50 mm.

The laser table supports a range of sub-mW CW diode lasers at different wavelengths (532, 635, 670, 780 and 808 nm). Several optical elements are used to achieve a tightly–focused laser beam, and beam profiles measured with a diagnostic camera placed at the equivalent working distance to the cathode show a beam size around 40 to 80 μm FWHM at the photocathode surface. A series of ND filters are used to control beam intensity. The laser beam is at grazing–incidence with respect to the photocathode under study, making an angle of 17° with the surface plane.

A PCO.2000 CCD camera captures images from the phosphor screen. The camera has a cooled 2048×2048 pixel array with a *Q.E.* around 50 % at the 543 nm peak emission wavelength of the phosphor screen. It boasts excellent low–noise performance, and has a 14-bit ADC giving a claimed dynamic range of 73 db (around 4,400:1 in practice). Imaging is delivered through a Tamron f 3.5 180 mm macro lens and several lens tube spacers to boost magnification. This combination delivers a spatial resolution of 18 μm/pixel in the recorded images. The camera and lens assembly are firmly anchored and vibration–free, so allowing long exposure times during data acquisition.

Experimental details

Commissioning measurements were performed on a p^+-GaAs(100) photocathode supplied by the ISP. To test the resolving power of the TESS system, we minimised the photoelectron energy spread by using photocathodes activated only to a state of positive electron affinity. The PPF was used to activate a GaAs photocathode following established procedures [6, 7], achieving about 2 % quantum efficiency under illumination at 635 nm. Once loaded into the TESS photocathode holder, it was illuminated with CW

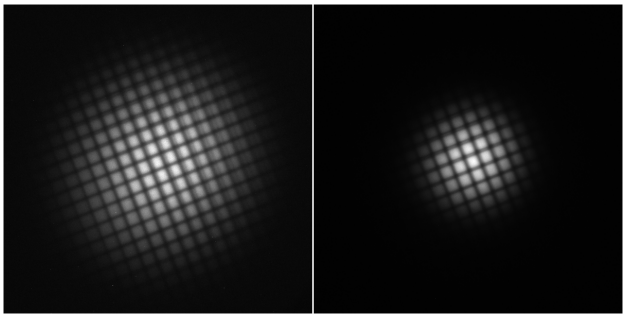

Figure 2: Electron emission footprint under illumination at $\lambda = 635\,\text{nm}$ with the retarding grid structure superimposed for $U_{acc} = 60\,\text{V}$ (**left**); and $U_{acc} = 230\,\text{V}$ (**right**).

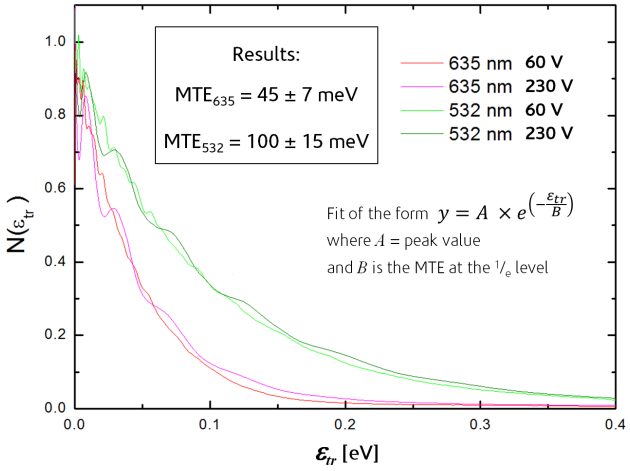

Figure 3: Measurements of transverse energy distribution curve and corresponding MTE for photoelectrons emitted from GaAs under illumination by red and green laser light.

laser light, firstly at a wavelength of 635 nm, and then later 532 nm. In both cases, the spot was focused to a size between 40 and 80 μm FWHM. Prior to making a measurement, the laser power delivered to the cathode was adjusted through the addition of ND filters to establish a measured drain current from the photocathode around 10 pA. During a measurement, additional ND filters were inserted increasing beam attenuation by 10^4 and pushing the extracted current into the 1 fA regime, thereby avoiding the effects of space–charge.

During data acquisition, the photocathode source was operated at either - 30 V or - 200 V, with the detector grids and the MCP front plate all held at the same potential of + 30 V. Changing the source voltage controls the effective accelerating potential (U_{acc}), and therefore the time of flight (τ) for the emitted electrons – a longer time of flight associated with a smaller overall accelerating voltage gives more time for the transverse energy component to act and thereby expand the footprint of the emitted electrons.

The MCP back plate was held at + 950 V, and the phosphor screen at + 3500 V. Images from the phosphor screen showing the electron emission footprint were acquired using camera exposures of 40 s, with extraneous light removed as far as possible. An emission image and a dark background image were taken in each case, and the dark image then subtracted to create a true image of the electron emission footprint. Four emission footprint images were measured, corresponding to the two different source voltages and the two different illumination wavelengths. Figure 2 shows the recorded beam footprints under illumination at $\lambda = 635\,\text{nm}$ prior to background removal.

Data analysis

With the background image subtracted, a histogram of the true image was generated which summed each column in the data set. By comparing the overlap of the X- histogram duly generated with its reversed form, adjusting their X-displacement as required to achieve coincidence, a check on data set symmetry was carried out verifying data quality. Analysis of the X- and Y- histograms was then applied to establish the image centroid, and a radial distribution function $I(r)$ was derived. The function $I(r)$ reflects the number of electrons incident in the annulus with radius r and thickness δr, with the radial displacement r of an electron from the position of the image centroid (where $r = 0$) being dependent on its transverse energy ε_{tr}.

The drift distance between the source and the detector was 43 mm, and the longitudinal accelerating potentials used were $U_{acc} = 60\,\text{V}$ and 230 V respectively. In both cases, $e \cdot U_{acc} \gg \varepsilon_{lon}$, so the effect of longitudinal energy content at the instant of emission can be ignored as this will have a negligible effect on the overall flight time. TEDC were calculated for each data set by converting the radial distribution function $I(r)$ to an energy distribution function $N(\varepsilon_{tr})$ based on the radial displacement from the central emission point during the flight time between the source and detector, and these were then normalised to the maximum value.

Results

The TEDCs measured for a positive electron affinity GaAs photocathode are shown in Figure 3. The curves have an exponential character, so the values of MTE were extracted from the spectra by fitting a curve of the form $y = A \times \exp(-\frac{\varepsilon_{tr}}{B})$, where A is the peak intensity and B is the MTE at the $\frac{1}{e}$ level.

The results indicate that the MTE of electrons emitted from a GaAs photocathode is $\text{MTE}_{635} = 45 \pm 7\,\text{meV}$ under illumination at 635 nm, rising to $\text{MTE}_{532} = 100 \pm 15\,\text{meV}$ under illumination at 532 nm.

In both cases, the MTEs exceed kT (around 25 meV at room temperature) due to significant contributions from 'hot' non–thermalised electrons, the magnitude of this effect being dependent on illumination wavelength. Figure 3 clearly shows the effect of illumination wavelength, with the MTE increasing dramatically when the incident photon energy was changed to the shorter wavelength. These experiments were carried out consecutively, so the degrada-

tion state of the photocathode was essentially the same in both cases, though the *Q.E.* will differ according to wavelength. For the red laser at 635 nm, $h\nu = 1.95$ eV, rising to $h\nu = 2.33$ eV for the green laser at 532 nm. It is the additional photon energy at 532 nm which increases the upper limit on transverse and longitudinal energy for photoemitted electrons, thereby increasing the MTE.

Our results are in good agreement with measurements published by the Cornell and Matsuba groups [8, 9].

FUTURE WORK

The largest single source of error in this measurement is linked to the precise value of the drift distance between the cathode source and the detector. This is difficult to establish due to the thickness of the gaskets at either end of the TESS vacuum chamber, and also due to the aggregation of mechanical tolerances in the design. This measurement will be carried–out by laser survey when the system is next opened for maintenance.

A theoretical model of the TESS experiment has been developed and is currently undergoing refinement. This will be used to explore the effects of angular source distribution and field inhomogeneity due perhaps to detector mis–alignment on the measured results.

Several new GaAs photocathodes will be prepared and loaded into the PPF, and a series of measurements carried out on these under various conditions. Their *Q.E.* will be degraded through controlled over–oxidisation using the piezo–electric leak valve, and measurements of the MTE made during this evolution. We plan to measure MTE over a range of illumination wavelengths, and we will investigate the effects of surface roughening and poor cathode preparation on MTE.

Integration of the TESS system with other equipment in the laboratory is planned through development of a vacuum suitcase, giving access to AFM, SEM, XPS and LEED to study photocathode surfaces in detail, and also allowing measurements to be carried out on metal photocathodes.

Future work will also utilise the source cooling capability to measure the MTE from metal photocathodes at cryogenic temperatures.

ACKNOWLEDGMENTS

ASTeC would like to acknowledge support for its photocathode research and development activities from the European Union under the FP7 EuCARD2 capacities programme (grant agreement # 227579).

The authors would like to acknowledge the assistance of Jacek Wychowaniec (University of Aberystwyth, Dept. of Physics) in the early commissioning of the TESS system.

REFERENCES

[1] B.L. Militsyn, I. Burrows, R.J. Cash, B.D. Fell, L.B. Jones, J.W. McKenzie, K.J. Middleman, H.E. Scheibler & A.S. Terekhov; Proc. IPAC'10, 2347-2349.

[2] L.B. Jones, R.J. Cash, N. Chanlek, B.D. Fell, J.W. McKenzie, K.J. Middleman & B.L. Militsyn; Proc. IPAC '11, 3185-87.

[3] D.H. Dowell, I.V. Bazarov, B.M. Dunham, K.Harkay, C. Hernandez-Garcia, R. Legg, H. Padmore, T. Rao, J. Smedley & W. Wan; NIM 'A' 622 (2010), 685697

[4] D.J. Bradley, M.B. Allenson & B.R. Holeman; J. Phys. D.: Appl. Phys. 10(1), 1977, 111-125

[5] Z. Liu, Y. Sun, P. Pianetta & R.F.W. Pease; J. Vac. Sci. Technol. B 23(6), 2005, 2758-2762

[6] W.E. Spicer & R.L. Bell; Pub. Astron. Soc. **84** 110 (1972).

[7] W.E. Spicer, Appl. Phys. **12**, 115 (1977).

[8] I.V. Bazarov, B.M. Dunham, F. Hannon, Y. Li, X. Liu, T. Miyajima, D.G. Ouzounov & C.K. Sinclair; Proc. PAC '07, 1221-1223

[9] S. Matsuba, Y. Honda, X. Jin, T. Miyajima, M. Yamamoto, T. Uchiyama, M. Kuwahara & Y. Takeda; Jap. J. Appl. Phys. 51 (2012), 046402